be distinguished from the $a_{1u}/a_{2u}$ thermal mixture.[50] Unfortunately, we failed to detect it for both $(TMP^{\bullet+})Fe^{III}(ClO_4)_2$ and $(TMP^{\bullet+})Fe^{IV}{=}O$. $(TPP^{\bullet+})Cu^{II}$ and $(TPP^{\bullet+})Fe^{III}Cl(SbCl_6)$ are known to adopt a ruffled structure in a crystal[52] and probably so in solution. In contrast, $(TMP^{\bullet+})M$ are considered to adopt a planar structure.[39,46,49] This feature and the hindrance of the torsion around the $C_m$–$C_{phenyl}$ bond stated above may suggest that the $(TMP^{\bullet+})M$ system gives more pure $a_{2u}$ radical than the $(TPP^{\bullet+})M$ system.

Since the $C_\beta C_\beta$ bond is antibonding and bonding for the $a_{1u}$ and $a_{2u}$ HOMOs, respectively,[51] removal of an electron from the $a_{1u}$ or $a_{2u}$ orbital is expected to cause the up- or downshift of the $C_\beta C_\beta$ stretching vibrations. On the other hand, the $C_\alpha N$ bond is nonbonding and antibonding for the $a_{1u}$ and $a_{2u}$ HOMOs;[51] the downshift of the $C_\alpha N$ stretching frequency is never expected upon formation of a cation radical from the simple consideration. This implies that significant configuration interaction occurs in the cation radical state and the resultant electronic state cannot be easily inferred from the ground-state wave functions of neutral porphyrins.

In conclusion, it became evident that both the $\nu_4$ and $\nu_2$ bands are shifted significantly to lower frequency in the $\pi$ cation radical of $Fe^{III}$ and $Fe^{IV}$ porphyrins. Little shift of the $\nu_4$ frequency upon the formation of compound I of HRP raises a question about the established assignment of the $\pi$ cation radical at ambient temperatures. The RR spectrum of oxoferryl porphyrin $\pi$ cation radical is along the extension of the $a_{2u}$-type divalent metalloporphyrin $\pi$ cation radicals, but it might be different from other $a_{2u}$-type $\pi$ cation radicals given by $(TPP^{\bullet+})M$ with regard to the torsion around the $C_m$–$C_{phenyl}$ bond. The $\nu_{Fe=O}$ frequency is not greatly perturbed by formation of the $\pi$ cation radical, but is more sensitive to its trans ligand. The controversy between Kincaid et al.[30] and our previous report[29] was reasonably explained in terms of the difference of the trans ligand.

(52) Scheidt, W. R. *Struct. Bonding (Berlin)* **1987**, *64*, 1-70.

# Porphyrin Sponges: Structural Systematics of the Host Lattice

**Marianne P. Byrn, Carol J. Curtis, Israel Goldberg,† Yu Hsiou, Saeed I. Khan, Philip A. Sawin, S. Kathleen Tendick,‡ and Charles E. Strouse***

*Contribution from the Department of Chemistry and Biochemistry, J.D. McCullough Crystallography Laboratory, University of California, Los Angeles, California 90024-1569.*
*Received November 7, 1990*

**Abstract:** Analysis of the crystal structures of over 100 tetraarylporphyrin-based lattice clathrates reveals the extent to which van der Waals interactions between host molecules govern the crystal packing. In all these materials, corrugated sheets of tightly packed porphyrin molecules stack to form arrays of parallel channels in which a remarkable variety of guest species are accommodated. Conservation of the host structure in the absence of any covalent or hydrogen-bonding connection between host molecules suggests an engineering strategy for the designed construction of molecular solids. This strategy is based on the use of rigid molecular building blocks with self-complementary shapes. Identification of the features of the molecular structure responsible for the versatility of tetraarylporphyrin-based clathrates lays the groundwork for the development of new microporous materials. X-ray structural data are provided for 34 new materials.

## Introduction

The utility of microporous solids in many scientific and technological applications has led to the development of several strategies for the designed construction of lattice clathrates. The host lattices targeted in these efforts include three-dimensional extended solids, networks of hydrogen-bonded molecules, and molecular solids in which only van der Waals forces maintain the host structure. The large class of tetraphenylporphyrin (TPP)-based clathrates previously identified in this laboratory[1] fall into the last category. In materials of this kind, control of the clathrate properties of the solid is based primarily on the control of molecular shape.

Although the clathrate properties of most molecular host materials (including the TPP-based hosts) have been discovered by chance, rational efforts in the design of new host systems have been successful. Notable in this regard is the work of MacNicol,[2] which focuses primarily on the maintenance of high symmetry in the molecular building blocks. Large rigid molecules of high symmetry have few degrees of conformational and orientational freedom and are thus unlikely to pack efficiently in a three-dimensional lattice. Any inefficiency in the packing produces a driving force for clathrate formation. Clathrate properties of many molecular materials can be rationalized on this basis. Among these are the Werner complexes,[3] the cyclophosphazenes,[4] perhydrotriphenylene,[5] the cyclotriveratrylenes,[6] the triphenylmethanes,[7] tri-*o*-thymotide,[8] numerous "hexa-hosts" prepared by MacNicol and co-workers,[2] as well as the "porphyrin sponges".[1] Tetraphenylporphyrin-based hosts differ in one important way from most of the others. While they do not pack efficiently in three dimensions, TPP molecules pack quite efficiently in two dimensions. As a consequence one finds in a large number of such clathrates a common host structure shown in Figure 1. This observation provides the basis for the development of a more controlled approach to the design of microporous molecular solids based on rigid symmetric building blocks with self-complementary shapes.

The investigation reported herein includes a detailed analysis of the molecular packing in over 100 TPP-based clathrates. This

* Author to whom correspondence should be addressed.
† School of Chemistry, Tel-Aviv University, Israel.
‡ Department of Chemistry, Harbor College, Los Angeles, CA.

(1) Byrn, M. P.; Curtis, C. J.; Khan, S. I.; Sawin, P. A.; Tsurumi, R.; Strouse, C. E. *J. Am. Chem. Soc.* **1990**, *112*, 1865-1874.
(2) MacNicol, D. D. *Inclusion Compounds*; Academic Press: New York, 1984; Vol. 2, Chapter 5.
(3) Lipkowski, J. *Inclusion Compounds*; Academic Press: New York, 1984; Vol. 1, Chapter 3.
(4) Allcock, H. R, ref 3, Chapter 8.
(5) Farina, M., ref 2, Chapter 3.
(6) Collet, A., ref 2, Chapter 4.
(7) Davies, J. E. D.; Finocchiaro, P.; Herbstein, F. H., ref 2, Chapter 11.
(8) Arad-Yellin, R.; Green, B. S.; Knossow, M.; Tsoucaris, G. *Inclusion Compounds*; Academic Press: New York, 1984; Vol. 3, Chapter 9.

0002-7863/91/1513-6549$02.50/0 

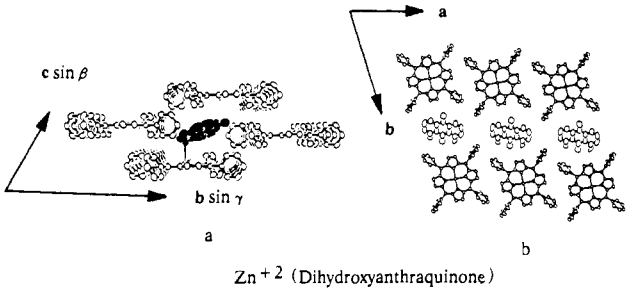


**Figure 1.** (a) A view down the channel of a typical porphyrin sponge. (b) A section parallel to *a* and *b*. In this and in subsequent figures, the porphyrin is tetraphenylporphyrin unless otherwise indicated.

analysis makes use of 45 new "porphyrin sponges", 34 of which have been recently prepared in this laboratory in the exploration of various applications. These new materials further illustrate the versatility of TPP-based clathrates.

## Experimental Section

**X-ray Measurements.** All X-ray measurements made use of locally automated Huber, Syntex, and Picker diffractometers equipped with graphite monochromatized Mo and Cu sources. The Huber diffractometer is equipped with a closed cycle Air Products refrigerator, and the Picker diffractometer is equipped with a gas stream low-temperature device. All crystals were coated with epoxy or grease to prevent loss of solvate and mounted on glass fibers. Crystallographic techniques used have been described previously.[9]

**Synthesis.** In most cases clathrates were prepared by recrystallization of the host from liquid guest. For high-melting guests, crystals were formed by cooling solutions of the host and guest in mesitylene, *p*-diisopropylbenzene, or benzene. All porphyrins were obtained from Midcentury Chemical (Posen, IL).

## Results

Lattice parameters of 45 new "porphyrin sponges" are tabulated in Table I. A more complete version of this table including all previously identified sponges is provided as supplementary material. Figure 2 illustrates the diversity in guest:host stoichiometry exhibited by these new materials. Clathrates containing from 1 to 5 guest molecules per host molecule are displayed. In the sponges with 1:1 stoichiometry (see also Figure 1), inversion disordered guest molecules[20] occupy the channel formed by chains of porphyrin molecules. The 2:1 stoichiometry, by far the most common, is represented by one sponge in which there are two inversion related guests and one in which two different guests occupy pseudo-inversion related sites.[21] The first material with 3:1 stoichiometry illustrates the fact that sponges based on tetratolylporphyrins can adopt structures very similar to those based on tetraphenylporphyrins. In both of the 3:1 clathrates, a disordered toluene molecule is located at an inversion center in the channel. The expanded repeat distance down the porphyrin chains exhibited by the first of two structures with 4:1 stoichiometry is seen for a number of other sponges (see Table 1b). The sponge containing bicycloheptenecarboxylic acid was prepared with the expectation that hydrogen-bonded dimers would be disposed about a crystallographic inversion center in the channel. Instead, an inversion related pair of hydrogen-bonded dimers was incorporated (O–O distances = 2.67 and 2.68 Å). The two structures with 5:1 stoichiometry both contain $SbX_6^-$ anions. In the second of these, as in one other material reported previously,[1] guests occupy channels along all three lattice directions (see Table Id).

Figure 3 shows the packing for nine sponges in which the guests have monosubstituted aromatic six-membered rings. In all but the last of these, the dispositions of the substituents are very similar. Other examples of these two structural types were observed previously.[1]

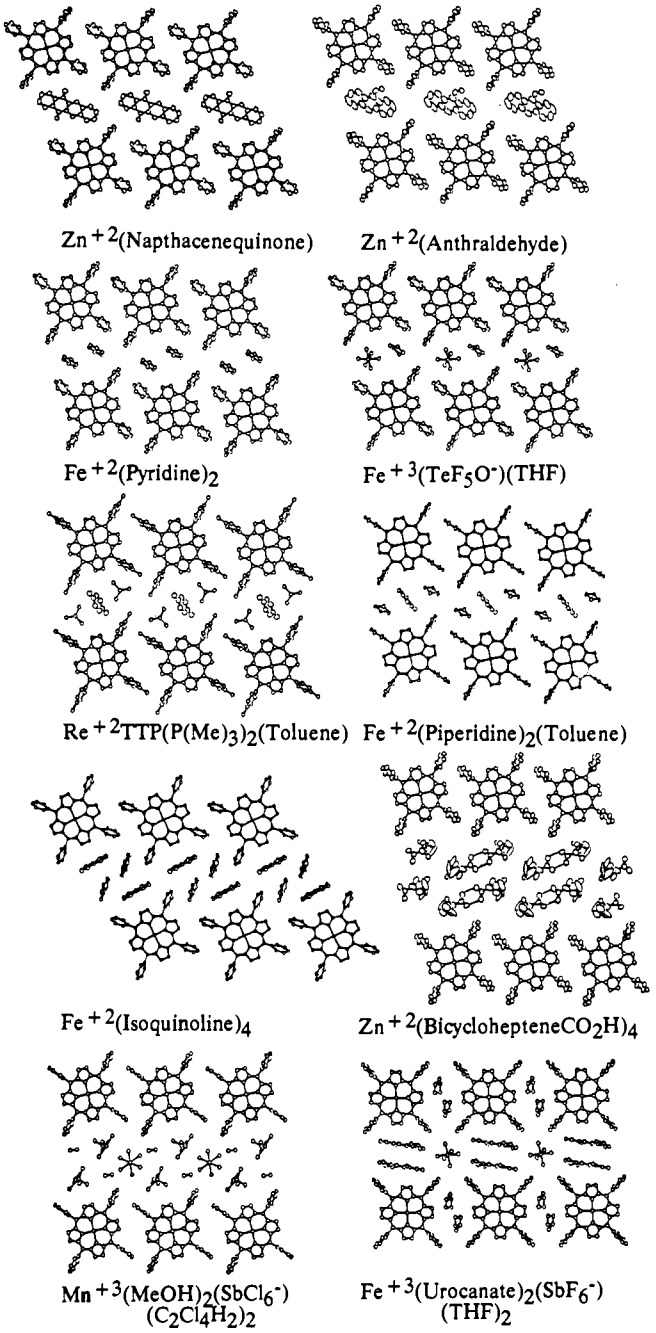


**Figure 2.** Porphyrin sponges with 1:1, 2:1, 3:1, 4:1, and 5:1 guest:host stoichiometry.

(9) Byrn, M. P.; Strouse, C. E. *J. Am. Chem. Soc.* **1991**, *113*, 2501–2508.
(10) Li, N.; Coppens, P.; Landrum, J. *Inorg. Chem.* **1988**, *27*, 482–488.
(11) Kellett, P. J.; Pawlik, M. J.; Taylor, L. F.; Thompson, R. G.; Levstik, M. A.; Anderson, O. P.; Strauss, S. H. *Inorg. Chem.* **1989**, *28*, 440–447.
(12) Sodano, P.; Simonneaux, G.; Toupet, L. *J. Chem. Soc., Dalton Trans.* **1988**, 2615–2620.
(13) Ball, R. G.; Domazetis, G.; Dolphin, D.; James, B. R.; Trotter, J. *Inorg. Chem.* **1981**, *20*, 1556–1562.
(14) Belani, R. M.; James, B. R.; Dolphin, D.; Rettig, S. J. *Can. J. Chem.* **1988**, *66*, 2072–2078.
(15) Ciurli, S.; Gambarotta, S.; Floriani, C.; Chiesi-Villa, A.; Guastini, C. *Angew. Chem., Int. Ed. Engl.* **1986**, *25*, 553–554.
(16) Li, N.; Petricek, V.; Coppens, P.; Landrum, J. *Acta Crystallogr.* **1985**, *C41*, 902–905.
(17) Scheidt, W. T.; Pearson, W. B.; Gosal, N. *Acta Crystallogr.* **1988**, *C44*, 927–929.
(18) Quinn, R.; Valentine, J. S.; Byrn, M. P.; Strouse, C. E. *J. Am. Chem. Soc.* **1987**, *109*, 3301–3308.
(19) Collman, J. P.; Garner, J. M.; Kim, K.; Ibers, J. A. *Inorg. Chem.* **1988**, *27*, 4513–4516.
(20) The disorder is incomplete. An order parameter has been included in the refinement procedure as described in ref 9.
(21) The latter structure was refined as noncentrosymmetric (i.e. completely ordered).
(22) The unit cells chosen for the unsolvated hosts are different than those chosen in ref 1.

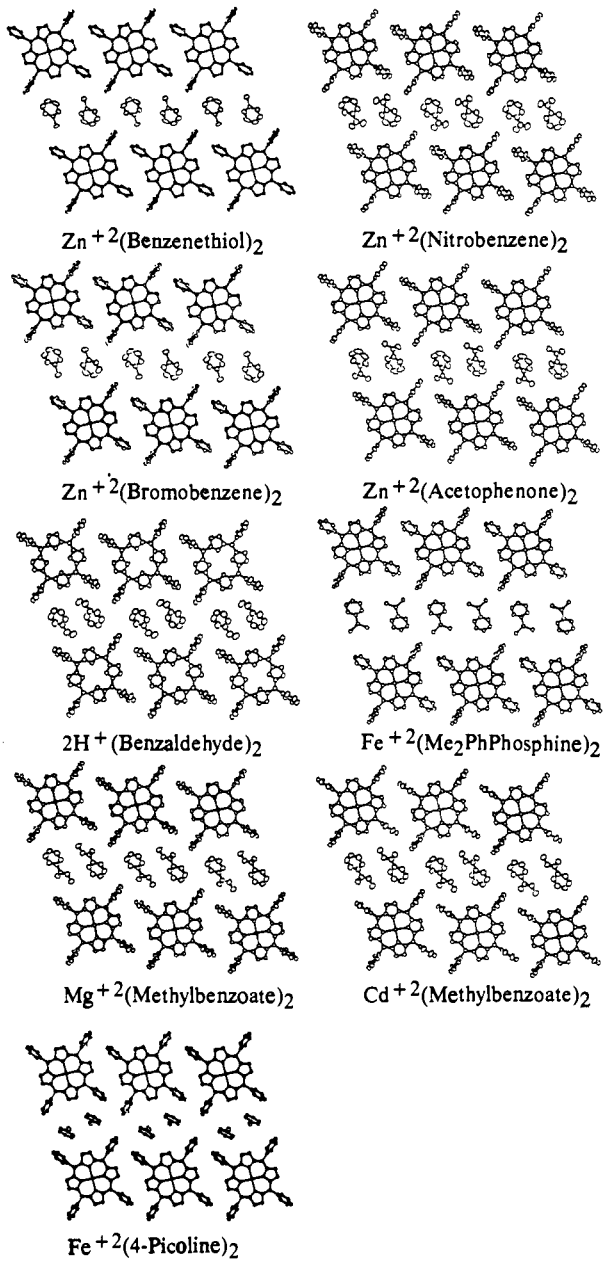


**Figure 3.** Porphyrin sponges with guests having monosubstituted six-membered rings.

Figure 4 shows the packing for sponges with ortho-subsituted benzene guests. These materials show three alternate substituent dispositions. The isopropylphenol structure exhibits intermolecular hydrogen bonding between guest molecules (O–O distance = 2.92 Å).

Clathrates containing 1,3- and 1,2,4-substituted benzene guests are shown in Figure 5. These structures fall into two classes. Those on the left exhibit the typical porphyrin repeat distance in the *a* direction of about 13.5 Å. Those on the right exhibit an "expanded *a*" and a "zigzag" channel, a mode of distortion observed previously.[1] Larger substituents seem to favor the "expanded *a*" arrangement. The *m*-hydroxyacetophenone structure exhibits intermolecular hydrogen bonding between inversion related molecules (O–O distance = 2.84 Å).

Figure 6 shows two sponges with para-substituted benzene guests. Para-substituted benzenes have been found to produce sponges with a variety of structures. ZnTPP crystallized from *p*-xylene ordinarily crystallizes with a 1:2 guest:host stoichiometry as opposed to the more common 2:1 packing mode. $H_2$TPP crystallizes from *p*-xylene with a 1:1 stoichiometry. The 2:1 ZnTPP clathrate shown here is thermodynamically unstable with respect to the 1:2 clathrate, but it can be produced as a kinetic

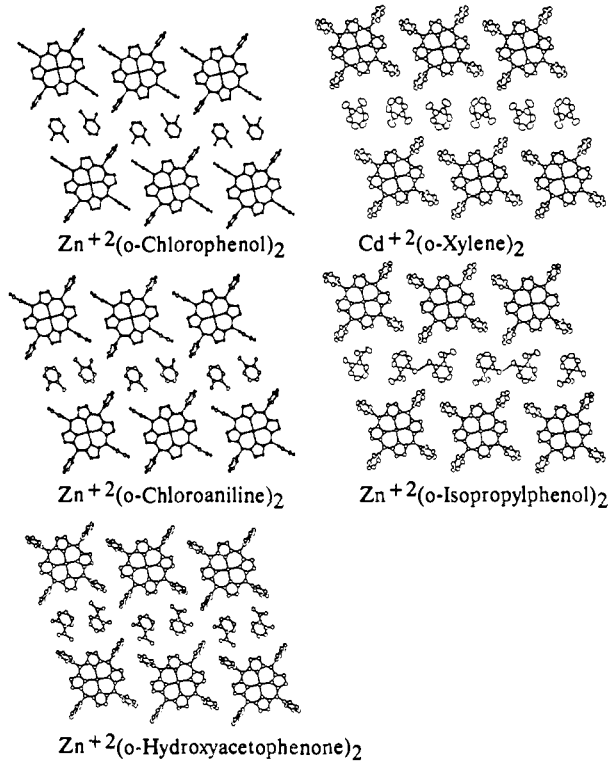


**Figure 4.** Porphyrin sponges with ortho-substituted benzene guests.

product by seeding a saturated solution with crystals of the 2:1 ZnTPP *o*-xylene clathrate.

Three sponges in Figure 7 contain double rows of guest molecules (see Table Ic). This double row structure is most commonly observed with guests having an elongated shape. Figure 8 shows views down the channel direction for "double row" clathrates based on 6-, 5-, and 4-coordinate porphyrins.

Figure 9 shows three sponges with large guest volumes and illustrates two different distortions of the sponge lattice that allow large guests to be accommodated. The first structure shows a typical *a* spacing of about 13.5 Å but a large $d_{002}$ spacing (the spacing between porphyrin-containing layers) of 6.6 Å. The other two structures show large *a* axis expansions and the "zigzag" channel structures but the more common $d_{002}$ spacing of about 4 Å. These materials demonstrate the extreme flexibility of porphyrin-based clathrates.

Figure 10 shows the structure of two 1:1 clathrates with bifunctional ligands chosen to link host molecules related by a *c*–*a* translation. The Zn–O distances are 2.58 and 2.50 Å for the anthrarufin and diacetylbenzene clathrates, respectively.

Figure 11 shows four sponges based on zinc tetra(4-methoxyphenyl)porphyrin (see sections e and f of Table I). The phenol and *m*-xylene clathrates contain a water molecule ligated to the Zn atom and hydrogen bonded to the methoxy groups of adjacent molecules. This hydrogen bonding represents another form of cross-linking. The *m*-cresol guests are also hydrogen bonded to methoxy groups, and the hydroxyacetophenone guests are coordinated to the zinc atom. Thus, 4-, 5-, and 6-coordinate complexes are represented in this group. While these materials differ in the nature of the hydrogen bonding and guest coordination, and while they adopt a variety of space groups, they all exhibit layered structures in which the packing within each layer is similar to that of the triclinic TPP-based sponges. Two of the 4-methoxyphenyl groups from each porphyrin segment the channel and create two types of potential guest sites. Both of these sites are occupied in the phenol–water and *m*-xylene–water clathrates, but only one is occupied in the *m*-cresol and *o*-hydroxyacetophenone clathrates.

Figure 12 shows the structures of triclinic unsolvated ZnTPP and $H_2$TPP in the unit cells tabulated in Table Ib. These unconventional unit cells[22] have equivalent positions $x, y, z$; $x, {}^1/_2 + y, z$; ${}^1/_2 + x, y, {}^1/_2 + z$; ${}^1/_2 + x, {}^1/_2 + y, {}^1/_2 + z$, and positions

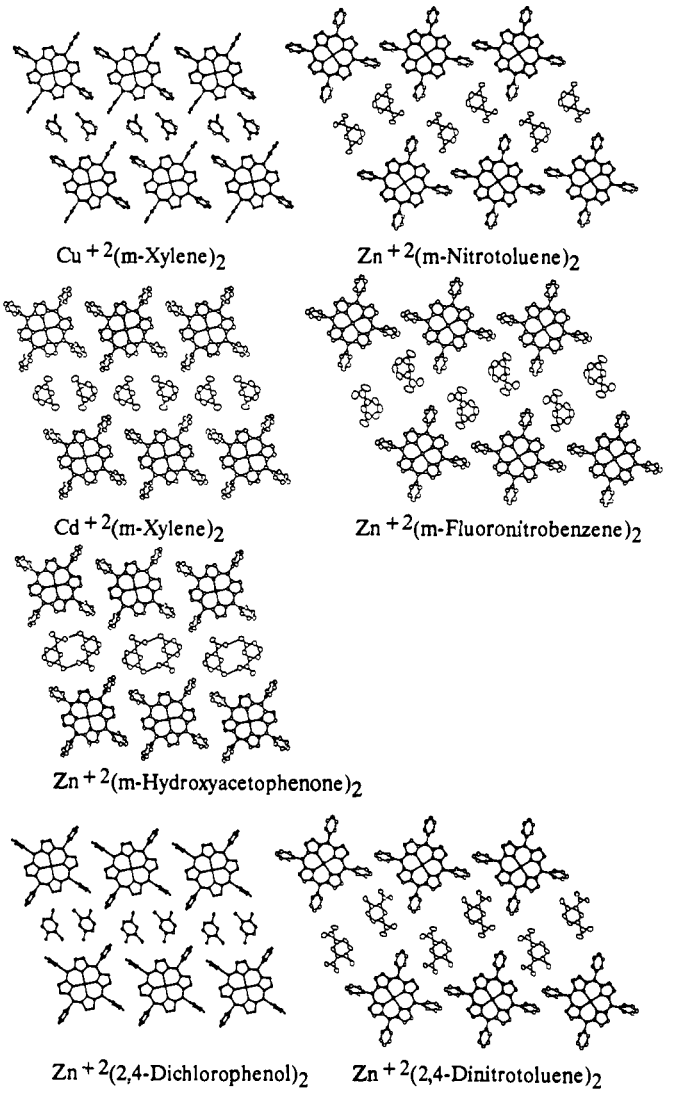


**Figure 5.** Porphyrin sponges with 1,3- and 1,2,4-substituted benzene guests.

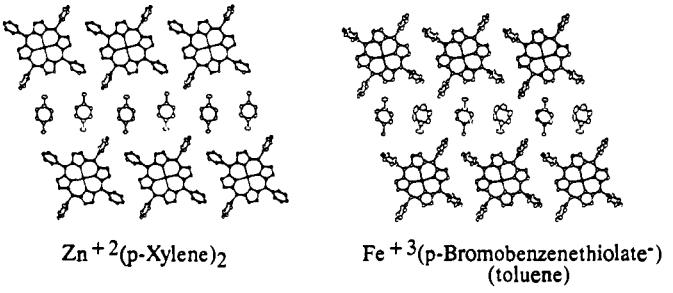


**Figure 6.** Porphyrin sponges with para-substituted benzene guests.

related to these by inversion. This choice of unit cell is useful because it provides a basis for comparing the stability of this material with that of the clathrates.

## Discussion

Nearly 100 "isostructural" triclinic porphyrin sponges have been identified. The guest species in these clathrates vary widely in molecular size, shape, and composition. The insensitivity of the host structure to the nature of the guests reflects the degree to which the packing in these clathrates is dominated by porphyrin–porphyrin interactions. Conservation of the solid-state host structure in this series is particularly striking as there are no hydrogen bonding or strong dipolar interactions between host molecules. This observation suggests that it may be possible to use the large base of experimental information available for these

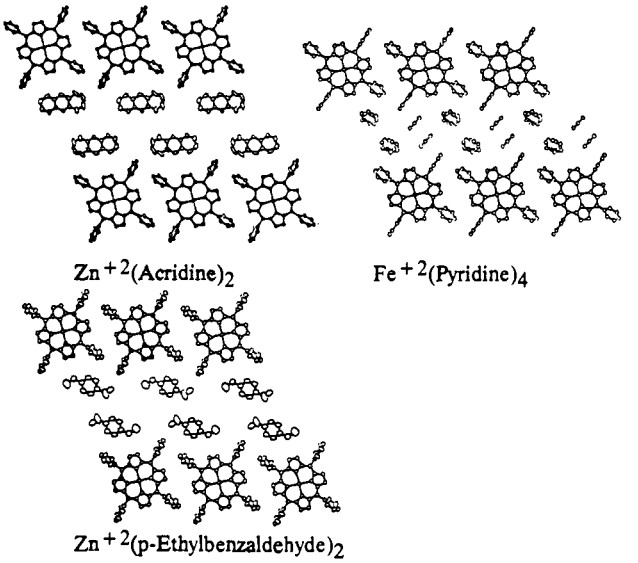


**Figure 7.** Porphyrin sponges with double rows of guests in the channel.

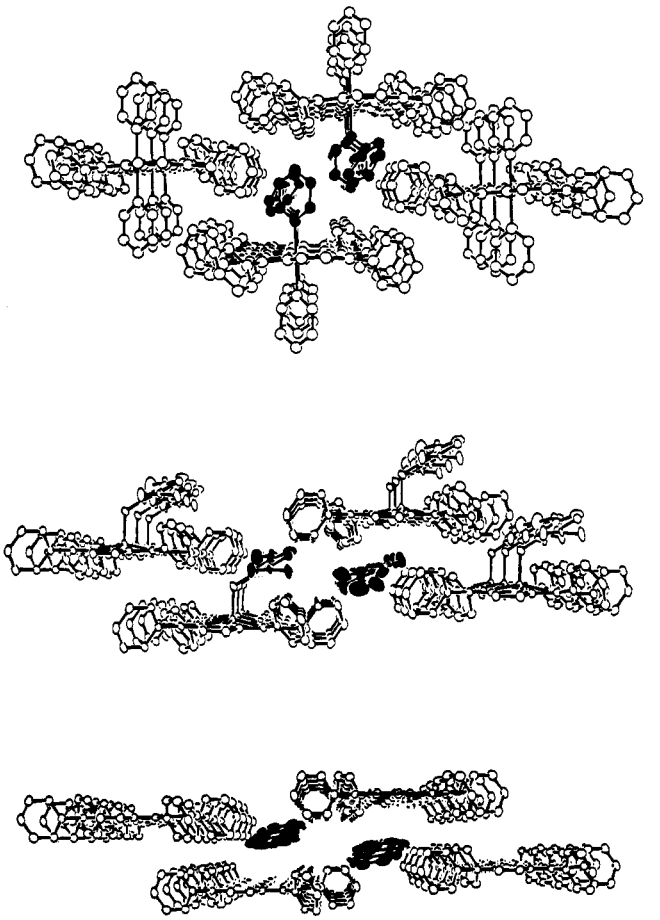

**Figure 8.** Double-row sponges based on 6-, 5-, and 4-coordinate TPP complexes.

clathrates to develop a general strategy for lattice design that could be applied to the construction of new microporous solids.

**Structural Systematics.** Because of the rigidity of the TPP molecules, and because of their lack of any polar or hydrogen-bonding substituents, relatively simple models can be used to rationalize their crystal packing. The crude mechanical models shown in Figure 13 are sufficient to explore van der Waals interactions between neighboring host molecules. Figure 13a shows that the surfaces of these molecules are "self-complementary" in the sense that coplanar molecules can pack very efficiently edge to edge. The interaction between perpendicular phenyl groups

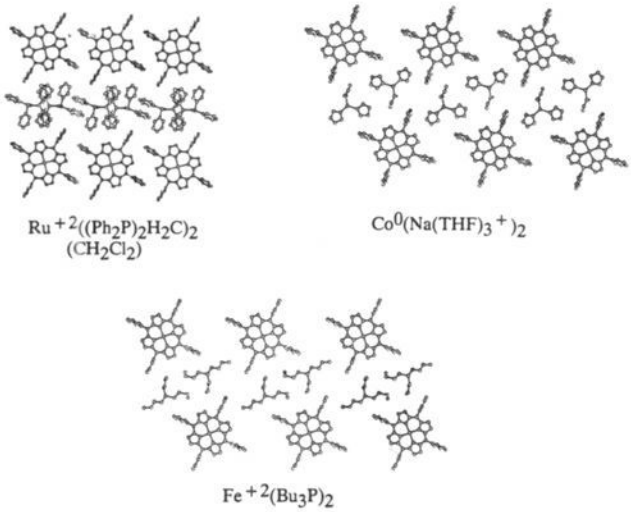


**Figure 9.** Porphyrin sponges with large unit cell volumes.

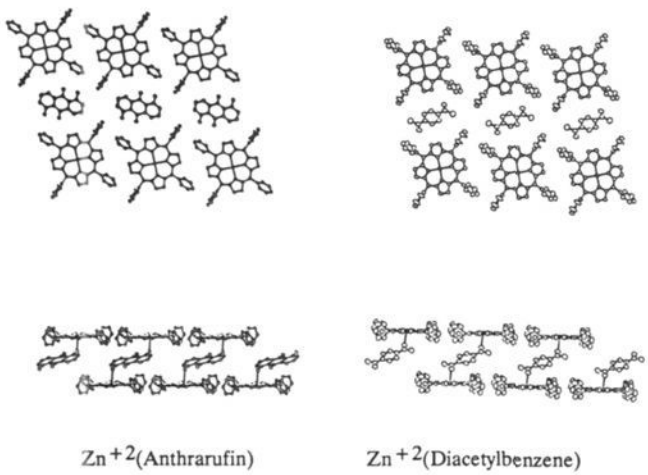


**Figure 10.** Porphyrin sponges containing "cross-linking" ligands.

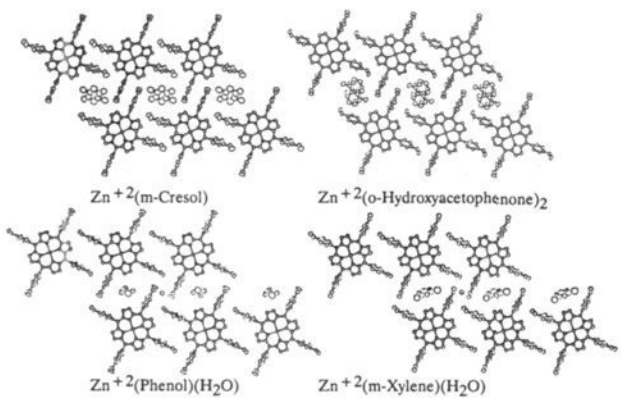


**Figure 11.** Sponges based on zinc(II) tetra(4-methoxyphenyl)porphyrin.

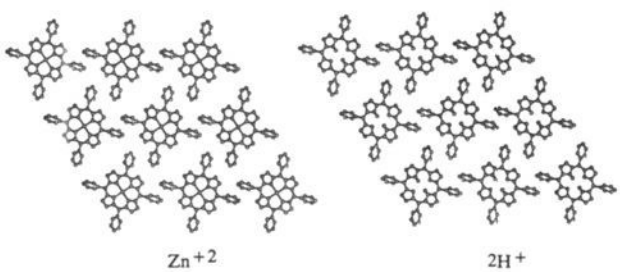


**Figure 12.** Unsolvated ZnTPP and $H_2$TPP.

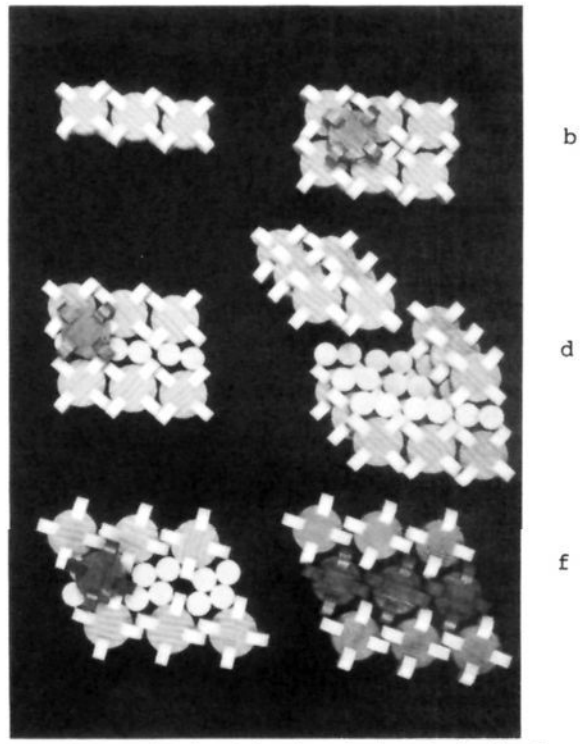


**Figure 13.** (a) A model of a chain of porphyrin molecules like those commonly observed in TPP-based clathrates, (b) two-dimensional tetragonal packing of porphyrin molecules, (c) intercalation of guests between two porphyrin chains, (d) guests intercalated between sheets of tightly packed porphyrin molecules, (e) an "expanded *a*" structure produced by a shear along the (1,0,−1) family of planes, (f) a representation of the unsolvated ZnTPP structure.

on adjacent molecules, similar to that in solid benzene,[23] further enhances the stability of this arrangement. The one-dimensional chain shown in Figure 13a, or a modified form described below, is found in all these triclinic sponges.

Because of the 4-fold molecular symmetry, this edge-to-edge packing arrangement can be extended into two dimensions to give the efficiently packed tetragonal arrangement shown in Figure 13b. If the packing of porphyrin molecules in the third dimension was equally efficient, there would be little driving force for clathrate formation. This is not, however, the case. The flat surface formed by the porphyrin cores is interrupted by mounds formed by sets of four convergent phenyl substituents. These mounds prevent efficient packing of a second layer of porphyrin molecules parallel to the first. The closest approach to efficient packing is achieved by matching the concave surface of a TPP molecule with each mound (see Figure 13b), but this arrangement does not result in good van der Waals contact between adjacent layers. This incompatibility can be viewed as the driving force for clathrate formation.

Tetragonal structures are observed only for porphyrins with very small axial ligands (see ref 1). These ligands fill the space between the layers, reducing the incompatibility.

Another way in which this incompatibility can be relieved is by division of each of the phenyl mounds into two smaller mounds. Incorporation of guest molecules between parallel chains of TPP molecules has exactly this effect (see Figure 13c). In porphyrin sponges, this incorporation (which reduces the symmetry from tetragonal to triclinic) preserves sheets of closely packed host molecules parallel to the (0,1,1) family of planes. When viewed this way, the inclusion of guests between parallel sheets represents a form of intercalation (see Figure 13d).

(23) (a) Bacon, B. E.; Curry, N. A.; Wilson, S. A. *Proc. R. Soc. London A* **1964**, *279*, 98–110. (b) Williams, D. E. *Acta Crystallogr.* **1980**, *A36*, 715–723.

**Table I.** Lattice Parameters for Tetraarylporphyrins[a,b]

| | space group | a | b | c | α | β | γ | vol | $d_{002}$ | ref |
|---|---|---|---|---|---|---|---|---|---|---|
| (a) "Normal" Triclinic Sponges | | | | | | | | | | |
| $Fe^{2+}$(pyridine)$_2$ | | 13.206 | 17.830 | 12.654 | 65.53 | 48.15 | 76.16 | (2017) | 4.41 | (10) |
| $Fe^{3+}$($TeF_5O^-$)(THF) | | 13.216 | 17.632 | 12.353 | 66.14 | 51.17 | 76.90 | (2049) | 4.51 | (11) |
| $Zn^{2+}$(4-diacetylbenzene) | | 13.433 | 17.943 | 13.369 | 61.26 | 48.86 | 79.03 | 2089 | 4.41 | tw |
| $Zn^{2+}$(anthrarufin) | | 13.367 | 19.988 | 11.825 | 59.69 | 50.61 | 71.47 | (2108) | 4.16 | tw |
| $Fe^{2+}$(4-picoline)$_2$ | | 13.287 | 17.796 | 12.969 | 65.45 | 50.14 | 76.16 | (2140) | 4.66 | tw |
| $Zn^{2+}$(1,8-$(OH)_2$anthraquinone) | | 13.406 | 20.292 | 12.142 | 59.80 | 49.68 | 72.10 | 2176 | 4.20 | tw |
| $Zn^{2+}$(*o*-chlorophenol)$_2$ | | 13.526 | 19.587 | 11.480 | 58.60 | 57.22 | 72.04 | (2181) | 4.33 | tw |
| $Zn^{2+}$(benzenethiol)$_2$ | | 13.472 | 20.918 | 11.952 | 59.30 | 49.15 | 70.77 | 2191 | 4.12 | tw |
| $Zn^{2+}$(9-anthraldehyde) | | 13.338 | 19.873 | 13.462 | 56.24 | 48.11 | 72.53 | 2194 | 4.34 | tw |
| $Zn^{2+}$(*o*-chloroaniline)$_2$ | | 13.626 | 19.838 | 11.560 | 58.56 | 55.96 | 71.93 | (2208) | 4.30 | tw |
| $Zn^{2+}$(2,4-dichlorophenol)$_2$ | | 13.417 | 20.111 | 11.302 | 57.72 | 59.14 | 72.48 | (2212) | 4.30 | tw |
| $Zn^{2+}$(bromobenzene)$_2$ | | 13.433 | 20.971 | 11.950 | 59.50 | 49.73 | 70.61 | 2213 | 4.16 | tw |
| $Cu^{2+}$(*m*-xylene)$_2$ | | 13.528 | 19.098 | 11.984 | 53.71 | 63.87 | 70.88 | (2231) | 4.57 | tw |
| $Fe^{3+}$(*p*-$BrPhS^-$)(toluene) | | 13.283 | 21.430 | 11.482 | 59.65 | 52.60 | 72.68 | (2240) | 4.12 | (9) |
| $Zn^{2+}$(5,12-naphthacenequinone) | | 13.871 | 20.940 | 13.205 | 56.61 | 44.56 | 68.25 | 2246 | 4.16 | tw |
| $Zn^{2+}$(nitrobenzene)$_2$ | | 13.559 | 20.791 | 12.333 | 57.10 | 50.55 | 70.44 | 2254 | 4.24 | tw |
| $Zn^{2+}$(*o*-hydroxyacetophenone)$_2$ | | 13.445 | 19.536 | 12.333 | 54.36 | 59.47 | 73.05 | 2268 | 4.51 | tw |
| $Zn^{2+}$(*p*-xylene)$_2$ | | 13.566 | 22.435 | 11.296 | 65.06 | 46.72 | 73.40 | 2269 | 3.89 | tw |
| $2H^+$(benzaldehyde)$_2$ | | 13.550 | 19.713 | 11.666 | 56.46 | 61.09 | 71.90 | 2270 | 4.47 | tw |
| $Zn^{2+}$(*m*-hydroxyacetophenone)$_2$ | | 13.436 | 22.094 | 11.416 | 64.25 | 48.98 | 73.98 | 2303 | 4.04 | tw |
| $Zn^{2+}$(acetophenone)$_2$ | | 13.523 | 20.129 | 12.325 | 54.43 | 58.43 | 71.50 | 2325 | 4.50 | tw |
| $Cd^{2+}$(*o*-xylene)$_2$ | | 13.807 | 22.109 | 11.085 | 66.97 | 48.52 | 73.03 | 2330 | 3.99 | tw |
| $Cd^{2+}$(*m*-xylene)$_2$ | | 13.563 | 21.970 | 10.995 | 65.76 | 51.55 | 72.55 | 2335 | 4.11 | tw |
| $Mg^{2+}$(methylbenzoate)$_2$ | | 13.482 | 21.235 | 12.480 | 56.62 | 51.97 | 69.65 | 2350 | 4.38 | tw |
| $Zn^{2+}$(*o*-isopropylphenol)$_2$ | | 13.874 | 21.611 | 11.561 | 65.98 | 48.52 | 74.77 | 2372 | 4.10 | tw |
| $Cd^{2+}$(methylbenzoate)$_2$ | | 13.518 | 21.212 | 12.514 | 55.03 | 54.11 | 69.89 | 2382 | 4.42 | tw |
| $Fe^{2+}$(dimethylphenylphosphine)$_2$ | | 13.698 | 22.980 | 11.149 | 67.87 | 47.66 | 74.53 | 2402 | 3.96 | (12) |
| $Fe^{2+}$(piperidine)$_2$(toluene) | | 13.346 | 18.440 | 11.772 | 66.12 | 67.01 | 84.28 | (2433) | 4.97 | tw |
| $Ru^{2+}$(($Ph_2P)_2Me)_2(CH_2Cl_2)$ | | 13.187 | 22.540 | 17.685 | 88.20 | 47.98 | 88.34 | 3903 | 6.57 | (13) |
| (b) "Expanded *a*" Triclinic Sponges | | | | | | | | | | |
| $Zn^{2+}$(*m*-fluoronitrobenzene)$_2$ | | 15.841 | 24.357 | 13.536 | 45.45 | 37.51 | 60.23 | 2245 | 3.35 | tw |
| $Zn^{2+}$(*m*-nitrotoluene)$_2$ | | 15.399 | 24.257 | 13.210 | 45.20 | 40.33 | 61.33 | (2248) | 4.43 | tw |
| $Zn^{2+}$(2,4-dinitrotoluene)$_2$ | | 16.228 | 24.913 | 13.771 | 43.73 | 40.07 | 61.89 | (2435) | 3.41 | tw |
| $Fe^{2+}$(isoquinoline)$_4$ | | 14.817 | 23.114 | 16.581 | 52.56 | 40.57 | 54.72 | (2858) | 5.11 | tw |
| $Fe^{2+}$(tri-*n*-butylphosphine)$_2$ | | 19.408 | 20.882 | 14.117 | 51.58 | 41.86 | 65.02 | 2982 | 4.06 | (14) |
| $Co^0(Na^+(THF)_3)_2$ | | 18.663 | 22.540 | 15.726 | 49.79 | 37.11 | 62.46 | 3029 | 4.06 | (15) |
| $Zn^{2+}$ | | 15.018 | 29.590 | 17.985 | 35.25 | 44.86 | 59.98 | 3192 | 4.15 | (1) |
| $2H^+$ | | 15.016 | 29.724 | 18.112 | 35.12 | 44.55 | 59.92 | 3195 | 4.14 | (1) |
| $Ag^{2+}$ | | 15.095 | 29.498 | 17.886 | 35.95 | 44.30 | 59.92 | 3206 | 4.16 | (1) |
| (c) "Double Row" Triclinic Sponges | | | | | | | | | | |
| $Zn^{2+}$(*p*-ethylbenzaldehyde)$_2$ | | 13.278 | 27.562 | 18.068 | 41.91 | 35.43 | 61.82 | 2402 | 3.72 | tw |
| $Zn^{2+}$(acridine)$_2$ | | 13.349 | 28.028 | 16.936 | 39.57 | 41.68 | 65.33 | (2490) | 3.66 | tw |
| $Fe^{2+}$(pyridine)$_4$ | | 13.546 | 20.821 | 18.097 | 85.72 | 30.77 | 94.11 | 2510 | 4.46 | (16) |
| $Mn^{3+}(MeOH)_2(SbCl_6^-)(C_2Cl_4H_2)_2$ | | 13.221 | 22.577 | 22.848 | 78.55 | 27.15 | 87.22 | 2922 | 4.90 | (17) |
| $Zn^{2+}$((bicycloheptene)$CO_2H)_4$ | | 12.751 | 28.145 | 22.863 | 63.94 | 27.24 | 77.80 | 3037 | 4.33 | tw |
| (d) "Multiple Channel" Triclinic Sponges | | | | | | | | | | |
| $Fe^{3+}$(Bzlm)$_2$($ClO_4^-$)(toluene) | | 17.826 | 17.145 | 11.967 | 78.96 | 49.47 | 81.13 | (2726) | 4.51 | (1) |
| $Fe^{3+}$(*t*-MeUro)$_2$($SbF_6^-$)(THF)$_2$ | | 15.343 | 18.983 | 14.267 | 71.45 | 49.21 | 85.01 | (2940) | 5.07 | (18) |
| (e) Substituted TPP Triclinic Sponges | | | | | | | | | | |
| $Zn^{2+}$(T(4-MeOPh)P(*o*-HO-Ace)$_2$ | | 14.413 | 20.288 | 20.051 | 48.09 | 37.04 | 56.44 | 2626 | 5.39 | tw |
| $Re^{2+}$(TTP($Me_3P)_2$(toluene) | | 14.173 | 19.392 | 12.191 | 69.41 | 59.02 | 85.02 | (2671) | 4.88 | (19) |
| $Fe^{3+}$(*o*-$NH_2$TPP)($PhS^-$)(PhSH) | | 13.478 | 21.178 | 11.684 | 61.57 | 50.60 | 71.36 | 2265 | 4.19 | (1) |
| (f) Substituted TPP Monoclinic Sponges | | | | | | | | | | |
| $Zn^{2+}$T(4-MeOPh)P(*m*-xylene)($H_2O$) | $P2_1/c$ | 15.157 | 18.967 | 24.522 | | 41.11 | | 4636 | | (1) |
| $Zn^{2+}$T(4-MeOPh)P(*m*-cresol)$_2$ | $P2_1/n$ | 14.672 | 9.675 | 15.713 | | 51.54 | | 2206 | | tw |
| $Zn^{2+}$T(4-MeOPh)P(phenol)$H_2O$ | $I2/c$ | 29.901 | 9.446 | 23.599 | | 41.64 | | 4429 | | tw |

[a] Unless otherwise noted, the porphyrin is tetraphenylporphyrin. For materials designated by "tw", structural data are provided with this report. Original references to structures analyzed in ref 1 are reported there. The unit cells chosen for the unsolvated materials at the end of section b are different than those chosen in ref 1. A volume in parentheses indicates a low-temperature structure determination. [b] Abbreviations: Ace, acetophenone; Bzlm, benzimidazole; Et, ethyl; $F_4$Ph, 2,3,5,6-tetrafluorophenyl; $Im^+$, imidazolium; Me, methyl; $NO_2$COHPhO, 2-nitro-5-formylphenolate; $F_4$Ph, 2,3,5,6-tetrafluorophenyl; *o*-$NH_2$TPP, tetraphenylporphyrinato with a single *o*-amino substituent; Ph, phenyl; PhEt(amine), phenethylamine; THF, tetrahydrofuran; TPP, tetraphenylporphinato; TTP, tetratolylporphinato; T(4-MeOPh)P, tetra(4-methoxyphenyl)porphinato; *t*-MeUro, *trans*-methylurocanate.

The body-centered triclinic unit cell in which the clathrates have been described was chosen such that the family of planes corresponding to the sheets of TPP molecules has the same Miller indices, (0,1,1), as it has in the body-centered tetragonal cell. The tetragonal arrangement of TPP molecules can be transformed to the arrangement found in the clathrates by a displacement of adjacent (0,1,1) sheets by $c/2$ (see Figure 14). On the basis of an initial tetragonal unit cell with $a$ = 13.5 Å and $c$ = 10.0 Å, such a displacement produces a triclinic unit cell with $a$ = 13.5 Å, $b$ = 21.3 Å, $c$ = 13.6 Å, $\alpha$ = 51°, $\beta$ = 46°, and $\gamma$ = 72°. These values correspond closely to the median values observed for the "normal" clathrates of $a$ = 13.5 Å, $b$ = 20.8 Å, $c$ = 11.9 Å, $\alpha$ = 62°, $\beta$ = 51°, and $\gamma$ = 73°. The differences between the hypothetical and observed values of $c$ and $\alpha$ can be attributed to a release of strain in the tetragonal structure upon separation of the (0,1,1) sheets.

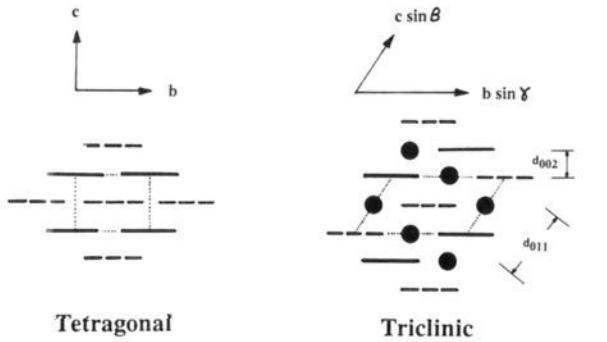


**Figure 14.** The relationship between the tetragonal and triclinic unit cells. The solid and dashed lines represent porphyrin molecules separated by $a/2$.

As shown in Figure 14, the $c/2$ displacement of adjacent sheets creates an array of channels parallel to $a$. The minimum height of the channels corresponds to the thickness of the porphyrin core and is thus ideal for the incorporation of organic (especially aromatic) guests.

**"Expanded a" Materials.** A major subclass of triclinic sponges is composed of materials with an "expanded" repeat distance in the $a$ direction ($a > 14$ Å) and an accompanying "zigzag" channel structure (see Table Ib and for example Figure 5). The "normal" structure can be transformed to the "expanded $a$" structure by a shear displacement along the (1,0,−1) family of planes. This shear removes the contact between two pairs of perpendicular phenyl groups along chains parallel to $a$ and creates a single new contact between parallel phenyl groups (see Figure 13e). In benzene dimers,[24] the offset stacked arrangement has been shown to have about the same stability as the T-shaped arrangement. The "expanded $a$" modification almost certainly has the effect of reducing overall porphyrin–porphyrin interactions, and most often occurs in cases where the guests constitute a large fraction of the cell volume. The shear displacement accounts for both the "expanded $a$" and the "zigzag" shape of the channel.

Noteworthy in this class are three materials with nitro-substituted guests. The fluoronitrobenzene, nitrotoluene, and dinitrotoluene clathrates have unusually small values of $d_{002}$, presumably associated with a strong cofacial $\pi$ donor/acceptor interaction between the stacked guest and host molecules. Previous investigators have addressed the significance of such interactions.[25] No interaction of this type is evident in the ZnTPP clathrate of nitrobenzene (see Table Ia).

**Sheet Structure.** Conservation of the two-dimensional sheets of TPP molecules in the absence of covalent or hydrogen-bonding linkages is surprising. It is obvious that efficient packing in the $a$ direction contributes to the stability of this arrangement, but the nature of the interaction between adjacent but non-coplanar molecules is less obvious. For this reason it is useful to explore the variations in the sheet structure exhibited by the sponges tabulated in Table I.

The translational symmetry operations that relate porphyrin molecules within each (0,1,1) sheet are the same in the triclinic and tetragonal cells. These can be described as combinations of $a$ and $(a + b - c)/2$ translations. In the "normal" TPP sponges, the $a$ lattice parameter is strongly conserved, varying from 13.2 to 13.9 Å. In the second direction there is somewhat more variation; Figure 15a depicts the relative disposition of molecules related by $(a + b - c)/2$. Although the guests do affect the sheet structure, the pattern produced reflects the predominant influence of porphyrin–porphyrin interactions. The $y$-shaped distribution in Figure 15a is clearly the result of interactions among the phenyl groups on adjacent molecules.

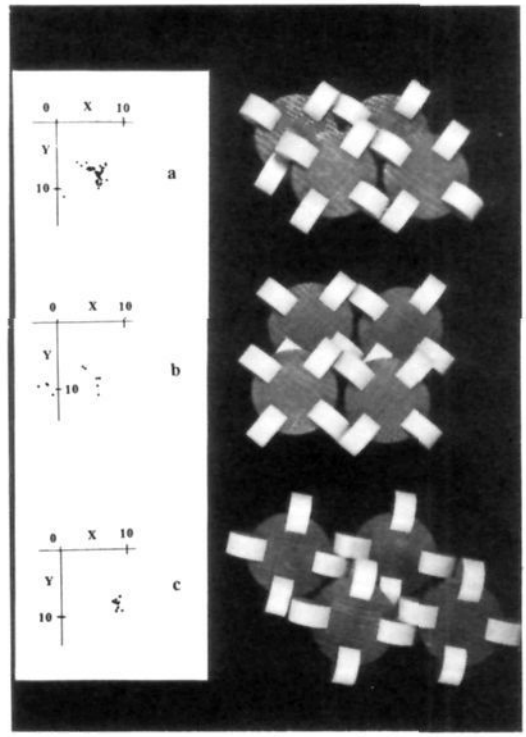


**Figure 15.** The relative disposition of host molecules related by $(a + b - c)/2$ in a coordinate system in which $X$ corresponds to the angstrom displacement in the $a$ direction and $Y$ is the angstrom displacement along $a \times (a \times b)$. Displacements for "normal" sponges are plotted in a, "double row" sponges in b, and "expanded $a$" sponges in c. The models have the same orientation and scale as the distribution plots. Model a represents the structure of the clump of materials in the left arm of the $y$, model b the materials with negative $X$, and model c a typical "expanded $a$" material. In terms of the models, the displacement being plotted is that of the left-most molecule in the top layer with respect to the left-most molecule in the bottom layer.

For "normal" TPP sponges there is a strong inverse correlation between the $d_{002}$ spacing and displacement along $Y$. Displacement away from the tetragonal structure ($X = 6.75$, $Y = 6.75$) in the direction of increasing $Y$ corresponds to a TPP molecule sliding off the edge of the two molecules beneath it and into the channel. This allows a decrease in $d_{002}$ (which corresponds to displacement *in the Z direction*).

The group of materials that make up the left arm of the $y$ in Figure 15a consists predominantly of materials in which the guest molecules are coordinated. The large $d_{002}$ of this sheet structure accommodates edge-on bonded ligands like pyridine, while the reduced value of $X$ makes the metal atoms more accessible to the guests.

The single observation significantly displaced from the $y$ is for a six-coordinate RuTPP complex with very large axial ligands; this structure has unusually large values of cell volume and $d_{002}$. The TPP sheet is so distended that the phenyl–phenyl interactions on adjacent molecules are no longer effective in controlling the sheet structure. The one-dimensional chain is, however, preserved ($a = 13.187$ Å).

The displacement of the $(a + b - c)/2$ molecule for the "double row" materials (see Figure 8 and Table Ic) is illustrated in Figure 15b. While the majority of these materials have sheet structures similar to the "normal" sponges, four of them exhibit structures with negative $X$. In these structures the sheets consist of more nearly square arrays of TPP molecules, as opposed to the more diamond shaped networks adopted by the "normal" sponges.

Figure 15c depicts the sheet structure in the "expanded $a$" materials. While there is more variation in the $a$ lattice parameter of these materials than observed for the "normal" sponges, there is somewhat less variation in the second dimension of the sheet.

Overall, there is considerable variation in the detailed structure of the TPP sheets, but the gross structure is strongly conserved;

(24) Jorgensen, W. L.; Severance, D. L. *J. Am. Chem. Soc.* **1990**, *112*, 4768–4774.

(25) (a) Williams, M. M.; Hill, C. L. *Inorg. Chem.* **1987**, *26*, 4155–4160 and references therein. (b) Walker, F. A. *J. Magn. Reson.* **1974**, *15*, 201–218.

**Table II.** Lattice Parameters of Clathrates of *m*-Xylene

| | *a* | *b* | *c* | $\alpha$ | $\beta$ | $\gamma$ | vol | $d_{002}$ | ref |
|---|---|---|---|---|---|---|---|---|---|
| $Cu^{2+}(m\text{-xylene})_2$ | 13.528 | 19.098 | 11.984 | 53.71 | 63.87 | 70.88 | (2231) | 4.57 | tw |
| $2H^{+}(m\text{-xylene})_2$ | 13.632 | 19.389 | 12.020 | 54.87 | 63.11 | 70.97 | 2308 | 4.62 | (1) |
| $Zn^{2+}(m\text{-xylene})_2$ | 13.464 | 21.709 | 11.174 | 64.80 | 51.98 | 72.99 | 2326 | 4.16 | (1) |
| $Cd^{2+}(m\text{-xylene})_2$ | 13.563 | 21.970 | 10.995 | 65.76 | 51.55 | 72.55 | 2335 | 4.11 | tw |

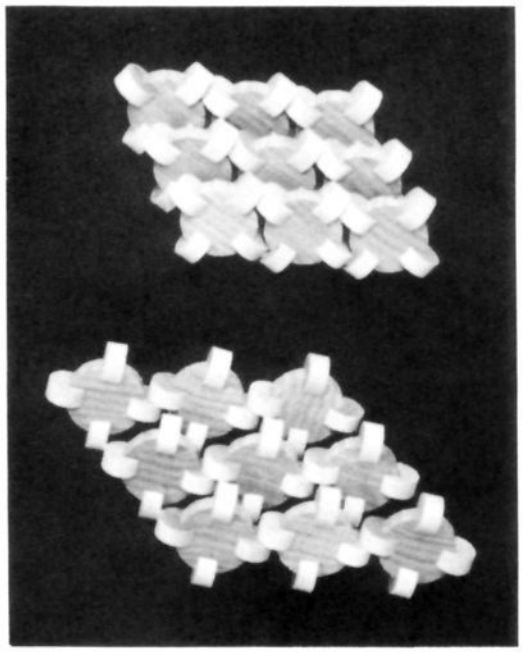

**Figure 16.** Models of the sheet structure in "normal" and "expanded *a*" sponges.

there is not a single low-energy arrangement, but a range of structures with very similar energies. This observation can be rationalized if the interactions between TPP molecules are divided into core–core, core–phenyl, and phenyl–phenyl interactions. The stability of the offset stacked arrangement of the large porphyrin cores[24] probably contributes significantly to the conservation of the sheet structure. This stability is largely insensitive to the detailed variation depicted in Figure 15. Likewise, interactions between phenyl groups and the porphyrin cores of adjacent molecules are likely to contribute to overall stability without being sensitive to relative displacement parallel to the porphyrin plane. Phenyl–phenyl interactions, on the other hand, are sensitive to such displacement and appear to account for the observed distributions. Because of the large size of the porphyrin core, however, there is still considerable flexibility in the relative dispositions of the phenyl groups.

In both the "normal" and "expanded *a*" materials, the surface properties of the TPP sheets determine the clathrate properties of the materials. Figure 16 shows the surfaces of "normal" and "expanded *a*" sheets. These rough surfaces are not self-complementary; only if the indentations in these surfaces are filled with guest molecules does efficient packing occur.

**Cross-Linked Sheets.** Two materials have been prepared in which the guests are bifunctional ligands chosen to link host molecules related by *c*–*a*. These ligands cross-link adjacent sheets of porphyrin molecules. The presence of a small amount of such a cross-linking agent in a clathrate containing other guests could have a significant effect on the clathrate properties. A small amount of cross-linker in a mother liquor may also serve to induce crystallization of the triclinic clathrate.

**Influence of the Metal Atom on Sheet Structure.** Although the nature of the metal atom might be expected to have a strong influence on host structure when the guest molecules act as ligands, it is somewhat surprising that the structures of clathrates with nonligating guests are sensitive to the identity of the metal atom. Examination of the four *m*-xylene clathrates for which structural data are available reveals relatively large structural variations. Lattice parameters for these four are summarized in Table II. The structure of the ZnTPP clathrate is similar to that of the CdTPP clathrate, and the structure of the $H_2$TPP clathrate is similar to that of the CuTPP clathrate, but these two pairs are quite different. The former materials have larger values of *b* and smaller values of $d_{002}$ (i.e. their channels are wider and more shallow). While it is difficult to assign this difference to a specific interaction, the structures of the Zn- and Cd-containing clathrates appear to reduce the interaction of the metal atom with phenyl groups on neighboring TPP molecules. Perhaps the larger size of these metals favors this arrangement. For any metal atom, these two different structures must have quite similar energies. This may account for the phase transitions that are observed occasionally when porphyrin sponges are cooled.

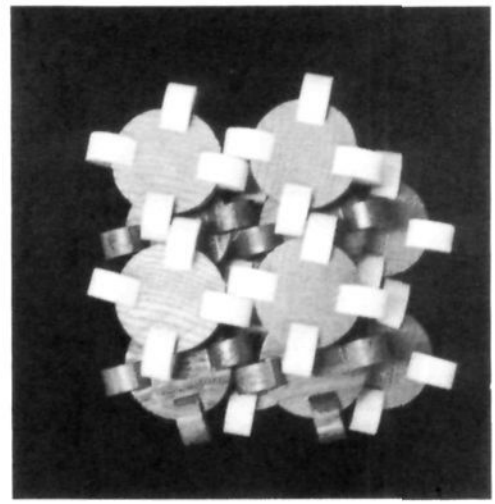

**Figure 17.** The structure of unsolvated TPP complexes with $I\bar{4}2d$ symmetry.

***Structures of the Unsolvated Hosts.*** A host material is likely to accommodate a wide range of guests only if the unsolvated host lattice is relatively unstable. It is thus of particular interest to examine the relationship between the structures of the clathrates and unsolvated hosts. The unsolvated form of ZnTPP, the most commonly used host in this investigation, can be prepared in a single-crystal form by crystallization from dichloromethane.[26] It is possible to choose a body-centered triclinic unit cell for this material that is very similar in size and shape to those for some of the larger clathrates with "expanded *a*" structures. In this cell the channels are occupied by porphyrin molecules (see Figures 12 and 13e). While this may seem a strange way to describe the structure, it provides the basis for comparison of the relative stability of the solvated and unsolvated materials. The porphyrin "guest" in the unsolvated material is a poor guest in the sense that it is large and rigid; it cannot adapt to the shape of the guest site.

It is instructive to examine the structures of unsolvated TPP complexes containing other metal atoms. While ZnTPP is triclinic, the Fe, Co, Ni, etc. analogues adopt the space group $I\bar{4}2d$. These structures[27] have an "expanded *a*" geometry in two dimensions. TPP molecules in one layer are centered over alternate pairs of phenyl groups in the layer beneath (see Figure 17). As in the case of the *m*-xylene clathrates, it appears to be the interaction

(26) Scheidt, W. R.; Mondal, J. U.; Eigenbrot, C. W.; Adler, A.; Radonovich, L. J.; Hoard, J. L. *Inorg. Chem.* **1986**, *25*, 795–799.
(27) Scheidt, W. R.; Lee, Y. J. *Struct. Bond.* (*Berlin*) **1987**, *64*, 1–70.

between the metal atom and the phenyl groups of adjacent molecules that prevents the zinc complex from adopting this more tightly packed structure. (The unit cell volume for NiTPP is 3152 Å$^3$ while that for ZnTPP is 3192 Å$^3$.) Destabilization of the $I\bar{4}2d$ structure by the $Zn^{2+}$ ion results in ZnTPP being much more soluble and in general a much better clathrate host than NiTPP.

There is another reason for interest in the structures of the unsolvated host. Preliminary investigations in this laboratory have revealed that removal of guests from many of the ZnTPP-based clathrates results in the formation of a material whose X-ray powder pattern is identical with that of the unsolvated material. Reintroduction of guests from the vapor phase produces clathrates with the same structures as those obtained by crystallization of the host from liquid guest. A more detailed account of this work will be provided elsewhere.[28]

**Lattice Clathrate Design.** Conservation of host structure in the large group of TPP-based clathrates examined herein demonstrates that *van der Waals interactions between rigid molecules with self-complementary shapes are sufficient to govern the solid-state structure.* This observation underlies a strategy for materials design based strictly on the control of molecular shape. Analysis of the large base of experimental information available for the TPP-based clathrates allows identification of those aspects of the TPP molecular structure that might be productively applied in the design of new molecular building blocks. These building blocks (the term is used here in a very literal sense) might then be used to "engineer" new materials with specific structures and properties.

Without doubt, the rigidity of the TPP molecule, which results from a high degree of conjugation, is essential to its function as an effective clathrate host. The only single bonds in the TPP molecule are those that connect the phenyl groups to the porphyrin core, and rotation about these bonds is severely restricted by interaction between the phenyl groups and the pyrrole hydrogen atoms.

Another essential feature of the TPP structure is its ability to pack efficiently in one or two but not all three dimensions. Close packing in two dimensions favors preservation of a common host lattice structure, while the inability to pack efficiently in three dimensions favors guest incorporation.

As a first step in the design of new microporous materials, it is useful to explore the effects of small modifications of the TPP structure on the clathrate structure. These modifications can be either those that are expected to enhance the stability of the clathrate structure or those that are expected to disrupt that structure. Both types of modifications could be useful in a systematic investigation.

At the present time only a relatively small amount of structural information is available for substituted TPP complexes. Most of the information that is available is for TPP complexes that have been substituted in the para position of the phenyl groups with either methyl or methoxy substituents. The set of methoxy derivatives in Figure 11 and the methyl derivative in Figure 2 provide some useful insight.

Para substitution might be expected to have a disruptive influence on the clathrate structure since it modifies the strongly conserved chain structure in the *a* direction. In all these materials, however, the chain structure is conserved as is the structure in the *b* direction. The structure in the third dimension, however, is disrupted, as reflected by the fact that the four methoxy-substituted clathrates exhibit four different space groups.

On the basis of examination of models, it would appear that 3,5-disubstitution of the phenyl groups should stabilize the structure of the TPP-based clathrates in that this substitution fills voids in the lattice and should improve van der Waals contact between host molecules. Studies of such materials are now underway.

More sophisticated modifications of TPP and the development of new non-porphyrin-based hosts will depend heavily on the use of more sophisticated forms of modeling. The utility of crude mechanical models in exploring the relationships among TPP clathrate structures suggests that modern molecular mechanics techniques will allow examination of subtle features of these structures and provide a more quantitative description of lattice energetics.

## Conclusion

Studies of tetraphenylporphyrin-based clathrates reported herein suggest the feasibility of a simple approach to lattice design based entirely on molecular shape. This approach is analogous to the "mortarless" construction of block walls, wherein the use of building blocks with interlocking shapes allows rapid construction of sturdy structures without the need for either mortar or skilled labor. Lego blocks and Lincoln Logs provide similar analogies. The key to success is in the design of the blocks. Through the design of rigid molecular building blocks with self-complementary shapes, one can envision construction of crystalline lattices with prescribed geometries. The design of lattice clathrates involves the use of blocks that are not entirely self-complementary, blocks that self-assemble leaving voids. Because tetraphenylporphyrin molecules are remarkably effective in this role, they function as prototype building blocks for the designed construction of microporous solids.

**Acknowledgment.** This work was supported by the National Science Foundation (CHE 87-06780) and the National Institutes of Health (GM 35329). We thank students in Chemistry 277 who participated in some of the research reported herein, and we thank Mr. William Minter for helpful discussions.

**Supplementary Material Available:** Listing of structural parameters for 34 materials, transformation matrices from the unit cells in which the structures were determined to the unit cells reported in Table I, and a version of Table I of lattice parameters including previously reported clathrates (156 pages). Ordering information is given on any current masthead page.

(28) Hsiou, Y.; Sawin, P. A.; Strouse, C. E. Manuscript in preparation.